doi:10.2478/enr-2026-0003

Circulating CXCL1 in newly diagnosed type 2 diabetes: context-dependent association with inflammatory load and metabolic indices

Ali Zeynettin [1], Orhan Balikci [2], Ozden Yildirim Akan [1], Erdi Dilaver [1], Ismail Demir [1]

[1]Department of Internal Medicine, University of Health Sciences, Izmir Bozyaka Training and Research Hospital, Izmir, Turkey; [2]Department of Internal Medicine, Izmir City Hospital Training and Research Hospital, Izmir, Turkey
E-mail: dralizeynettin@gmail.com

Objective. Metabolic syndrome (MS) and type 2 diabetes mellitus (T2DM) share a chronic low-grade inflammatory milieu driven by adiposity. C-X-C motif chemokine ligand 1 (CXCL1) has been linked to insulin resistance and endothelial dysfunction, but its diagnostic relevance remains unclear.

Methods. Our study employed a cross-sectional design and enrolled 104 adults: 52 newly diagnosed treatment-naive T2DM patients and 52 normoglycemic controls matched for age and sex. Serum CXCL1, high-sensitivity C-reactive protein (hs-CRP), and metabolic parameters were measured. Logistic regression models to discriminate MS and T2DM status were constructed (base model: age, sex, BMI) and then expanded by adding hs-CRP, CXCL1, or both. Model performance was assessed for discrimination (AUC), calibration (Integrated Calibration Index [ICI], Expected Calibration Error [ECE]), and clinical utility (decision curve analysis, DCA) in accordance with TRIPOD 2024.

Results. CXCL1 correlated with BMI (r=0.33, q=0.004) and hs-CRP (r=0.29, q=0.021), but not glycemic indices. For MS, CXCL1 marginally improved the base model (ΔAUC=+0.003, p=0.81); for T2DM, ΔAUC=+0.007 (p=0.60). hs-CRP performed better (AUC=0.744 for T2DM; 0.743 for MS) and the combined panel achieved the highest discrimination (AUC=0.769 and 0.745, respectively).

Conclusions. CXCL1 reflects adiposity-related inflammation but provides only minimal incremental discrimination for metabolic syndrome and T2DM beyond conventional markers such as age, sex, BMI, and hs-CRP. The combined hs-CRP+CXCL1 panel achieved the best overall statistical performance, although its clinical utility remains limited. These findings emphasize the need for integrated multi-marker approaches rather than single-biomarker screening in metabolic risk assessment.

Keywords: CXCL1, type 2 diabetes mellitus, metabolic syndrome, inflammation; hs-CRP, biomarker modeling, decision curve analysis

Type 2 diabetes mellitus (T2DM) is marked by insulin resistance and beta-cell dysfunction. Its prevalence continues to rise globally and it clusters with obesity and the metabolic syndrome (MS), a core cardiometabolic risk state (Sun et al. 2022). MS is defined by the co-occurrence of abdominal obesity, dyslipidemia, hypertension, and impaired glucose tolerance and it increases cardiovascular mortality (Eckel et al. 2005). Chronic low-grade inflammation is a defining component of the pathogenesis of both T2DM and MS (Guria et al. 2023; Pellegrini et al. 2024). In adipose tissue, macrophage infiltration

Corresponding author: Ali Zeynettin, M.D., Department of Internal Medicine, University of Health Sciences, Izmir Bozyaka Training and Research Hospital, Izmir, Turkey; phone: +90 507 921 5185; e-mail: dralizeynettin@gmail.com.

and pro-inflammatory mediators disrupt insulin signaling and metabolic homeostasis (Wu and Ballantyne 2020; Guria et al. 2023). Chemokines help orchestrate immune-cell trafficking in this setting and sustain crosstalk between inflammation and metabolism (Zlotnik and Yoshie 2000; He et al. 2024).

C-X-C motif chemokine ligand 1 (CXCL1) is an ELR-positive CXC chemokine that primarily regulates neutrophil chemotaxis and participates in inflammation and angiogenesis (Korbecki et al. 2022; Lazennec et al. 2024). The observational and experimental data suggest potential links between CXCL1 and obesity, T2DM, and microvascular complications (Sajadi et al. 2013; Korbecki et al. 2022; Monickaraj et al. 2023; Pan et al. 2024). Whether CXCL1 provides an independent associative signal beyond simple clinical variables such as age, sex, and body-mass index (BMI) remains uncertain (Wu and Ballantyne 2020; Korbecki et al. 2022).

Biological background and rationale: CXCL1 (GRO-alpha) signals mainly via CXCR2 activating ERK/MAPK, PI3K/Akt, and NF-κB pathways (Korbecki et al. 2022; Lazennec et al. 2024). It is produced by epithelial and endothelial cells, fibroblasts, adipocytes, and tissue macrophages, and is upregulated by interleukin-1β (IL-1β) and tumor necrosis factor-α (TNF-α) (Lo et al. 2014; Korbecki et al. 2022).

As a mediator of adipose-tissue, low-grade inflammation, CXCL1 is biologically linked to the obesity-insulin resistance axis (Wu and Ballantyne 2020). Experimental and clinical findings show higher CXCL1 in obesity/hyperglycemia phenotypes and inducible release during adipocyte differentiation via nuclear factor kappa-B (NF-κB) (Shaw et al. 2021).

From a translational perspective, single-analyte biomarkers such as CXCL1 may not outperform integrative inflammatory indices. However, their context-specific dynamics may still illuminate mechanisms underpinning metabolic risk. CXCL1 is usually measured by ELISA in serum or plasma and pre-analytical variables (freeze-thaw cycles, kit/lot differences, matrix effects) can influence results (Liu et al. 2021). We sought to characterize the association of serum CXCL1 with T2DM/MS and with core metabolic indicators (anthropometry, lipid profile, glycemic markers). We also quantified the incremental value of adding CXCL1 to a simple clinical model (age, sex, BMI) with high-sensitivity C-reactive protein (hs-CRP) across discrimination, calibration, and clinical utility. To ensure methodological transparency, reporting and analysis followed TRIPOD 2024 recommendations emphasizing both discrimination and calibration assessment (Collins et al. 2024).

Materials and Methods

Subjects. Our cross-sectional case-control study was conducted at the Department of Internal Medicine, Izmir Bozyaka Training and Research Hospital (University of Health Sciences), Izmir, Turkey, between January and December 2023. The protocol was approved by the institutional ethics committee (Approval No. 2023/107, 16 August 2023) and was carried out in accordance with the Declaration of Helsinki (2013 revision). Written informed consent was obtained from all participants prior to inclusion. The study enrolled 104 adults: 52 newly diagnosed, treatment-naive patients with T2DM and 52 normoglycemic control subjects matched by age and sex at a 1:1 ratio. Exclusion criteria included the presence of acute or chronic infection, autoimmune or malignant disease, hepatic or renal insufficiency, and use of any glucose-lowering, lipid-lowering, or systemic anti-inflammatory medication within the previous three months. Frequency matching was applied for age and sex, whereas BMI was not matched to preserve its variability for modeling.

Demographic, anthropometric and clinical parameters. All clinical and anthropometric measurements were obtained in the morning following an overnight fast of 8–12 h. Participants were asked to avoid smoking and caffeine for at least 30 min and to avoid strenuous exercise for at least 24 h before sampling. Weight and height were measured in light clothing and without shoes using a calibrated scale and stadiometer and BMI was calculated as weight (kg) divided by height squared (m^2). Waist circumference was measured midway between the lower costal margin and the iliac crest at the end of a normal expiration using a non-stretchable tape. Blood pressure was measured in the seated position after 5 min of rest using an automated sphygmomanometer and the mean of two readings was recorded. Demographic and lifestyle data were obtained via standardized interviews. Family history of T2DM was not systematically recorded in the control group and therefore was not included as a covariate.

Biochemical parameters. Venous blood samples were collected between 08:00 and 10:00 a.m. after fasting. Serum and plasma were separated within one hour by centrifugation at 3,000 rpm for 10 min at 4°C. Samples were aliquoted into polypropylene tubes, stored at −80°C, and subjected to a single freeze-thaw cycle to minimize pre-analytical variation. Fasting

plasma glucose, lipid profile, creatinine, urea, and liver enzymes were analyzed on an Abbott Architect c16000 platform using standard enzymatic methods. Glycated hemoglobin (HbA1c) was determined by high-performance liquid chromatography (HPLC) (Bio-Rad D-10). Insulin was quantified by electrochemiluminescence immunoassay (Roche Cobas e411) and insulin resistance was calculated by the homeostatic model assessment (HOMA-IR = [fasting glucose×fasting insulin]/405). hs-CRP was measured by immunoturbidimetry. Serum CXCL1 concentrations were determined in duplicate using a commercially available sandwich enzyme-linked immunosorbent assay (ELISA) (Human GROα/CXCL1 Kit, Elabscience, Cat. No. E-EL-H0045). The assay's analytical characteristics were as follows: sensitivity 7.8 pg/mL, linear range 15.6–1000 pg/mL, intra-assay coefficient of variation (CV) 6.8%, and inter-assay CV 8.9% consistent with the manufacturer's performance specifications. All assays were performed in blinded fashion by a single operator to minimize inter-assay variability, and internal QC samples showed <10% deviation after one freeze–thaw cycle.

T2DM diagnosis. T2DM was diagnosed according to the American Diabetes Association (ElSayed et al. 2023) criteria as fasting glucose ≥126 mg/dL and/or HbA1c ≥6.5%. MS was defined using the Joint Interim Statement (Alberti et al. 2009) requiring at least three of the following components: increased waist circumference (ethnic-specific cutoffs), triglycerides ≥150 mg/dL or treatment, reduced high-density lipoprotein-cholesterol (HDL-C) (<40 mg/dL in men, <50 mg/dL in women) or treatment, blood pressure ≥130/85 mmHg or antihypertensive therapy, and fasting glucose ≥100 mg/dL or T2DM.

Statistical analysis. Individual components of the syndrome were not included as separate covariates in the regression models to prevent information leakage. Continuous variables were winsorized at the 1st and 99th percentiles to mitigate outlier influence and standardized (z-scores) before multivariable analysis. Distribution normality was assessed by the Shapiro-Wilk test. Group comparisons employed independent-sample t-tests for normally distributed variables or Mann-Whitney U tests for skewed data and categorical variables were compared using chi-square or Fisher's exact tests. Effect sizes were expressed as Hedges g and multiple testing was corrected by controlling the false discovery rate (FDR) with the Benjamini-Hochberg procedure ($q<0.05$ considered significant).

To assess the incremental discriminative and clinical utility of CXCL1, four nested models were evaluated for each endpoint: base (age, sex, BMI); base+hs-CRP; base+CXCL1; and the full panel including both hs-CRP and CXCL1. Interaction terms for CXCL1 x BMI, CXCL1 x sex, and CXCL1 x hs-CRP were pre-specified and tested. Discrimination was quantified by the area under the receiver operating characteristic curve (AUC) with 95% confidence intervals derived by bootstrapping (2,000 resamples). To limit optimism bias, 5-fold stratified cross-validation was applied and the mean cross-validated AUC (CV-AUC) was reported. Calibration was evaluated by the Brier score, calibration intercept, and slope. The model reliability was further assessed through calibration plots comparing predicted and observed risk (apparent vs. bootstrap-corrected). Decision curve analysis was performed to examine net benefit across 10–30% intervention thresholds; net benefit is summarized at 10%, 20%, and 30% thresholds (Table 3). Thresholds of 10–30% were chosen based on the American Diabetes Association (ADA) and the International Diabetes Federation (IDF) criteria reflecting typical intervention ranges in metabolic screening, where TP and FP denote true and false positives, respectively, and pt represents the decision threshold. Integrated Calibration Index (ICI) and Expected Calibration Error (ECE) were additionally computed to provide complementary measures of model calibration.

To ensure robustness, sensitivity analyses were performed excluding participants with hs-CRP >10 mg/L (possible acute inflammation) and by stratifying results across hs-CRP tertiles. All analyses adhered to TRIPOD 2024 and the analysis plan was specified a priori to minimize analytic bias. Secondary analyses explored the relationship between CXCL1 and continuous metabolic indices (BMI, HOMA-IR, lipids) using Spearman's rank correlation and partial correlation adjusted for age, sex, and BMI. Variance inflation factors were checked to exclude multicollinearity. All analyses were conducted in R v4.3.2 (packages rms, pROC, rmda) and Python v3.11 (packages scikit-learn, statsmodels, pandas).

Results

A total of 104 participants were analyzed (52 newly diagnosed, treatment-naive T2DM and 52 normoglycemic controls). Age and sex distributions were comparable between the groups (Table 1).

As expected, participants with T2DM had higher adiposity (BMI; $p=0.002$) and a modestly higher resting heart rate ($p=0.03$), whereas waist circumference and blood pressure were similar. Glycemic

Table 1
Basic demographic, clinical, and laboratory characteristics (Control vs T2DM)

Variable	Control		T2DM		Test	p-value	Hedges g	q (BH)
	N	Value	N	Value				
Sex (Female/Males)	52	26 (50.0%)/ 26 (50.0%)	52	25 (48.1%)/ 27 (51.9%)	Chi-square	0.844	–	0.893
Age (years)	52	44.50 [40.00–47.75]	52	43.00 [41.75–50.00]	U	0.86	-0.126	0.893
Height (cm)	52	170.00 [164.50–175.00]	52	166.00 [158.75–175.00]	U	0.3	-0.257	0.451
Weight (kg)	52	78.13±15.85	52	81.35±11.19	t	0.236	0.232	0.398
BMI (kg/m^2)	52	26.93 [22.98–30.36]	52	29.71 [26.50–32.74]	U	0.002	0.566	0.011
Waist circumference (cm)	52	91.00 [83.75–98.00]	52	93.00 [82.75–97.25]	U	0.907	0.04	0.907
Heart rate (beats/min)	52	75.13±6.06	52	77.69±5.78	t	0.03	0.429	0.081
Systolic BP (mmHg)	52	128.50 [122.75–132.25]	52	126.50 [121.75–134.00]	U	0.735	0.044	0.827
Diastolic BP (mmHg)	52	77.00 [73.00–81.00]	52	75.00 [70.00–79.25]	U	0.08	-0.39	0.155
Fasting glucose (mg/dL)	52	89.00 [83.75–92.05]	52	132.00 [111.38–154.32]	U	<0.001	2.043	<0.001
Postprandial glucose (mg/dL)	52	101.50 [87.70–112.00]	52	223.00 [166.80–262.85]	U	<0.001	2.324	<0.001
Insulin (μIU/mL)	52	10.39 [6.97–15.16]	52	12.72 [11.29–19.74]	U	0.022	0.456	0.065
HOMA-IR	52	2.32 [1.60–3.69]	52	4.76 [3.21–7.32]	U	<0.001	–	<0.001
BUN (mg/dL)	52	26.10 [21.90–30.40]	52	26.40 [21.20–34.27]	U	0.405	0.26	0.521
Creatinine (mg/dL)	52	0.77 [0.70–0.81]	52	0.73 [0.65–0.82]	U	0.332	-0.188	0.472
AST (U/L)	52	16.75 [15.00–20.23]	52	15.00 [14.00–20.40]	U	0.185	-0.042	0.334
ALT (U/L)	52	17.25 [14.00–21.90]	52	18.50 [13.17–27.75]	U	0.273	0.293	0.434
LDH (U/L)	52	153.27±25.76	52	156.85±23.46	t	0.461	0.144	0.541
LDL-C (mg/dL)	52	115.37±22.04	52	124.01±23.00	t	0.053	0.381	0.12
HDL-C (mg/dL)	52	51.00 [43.50–58.25]	52	43.00 [34.00–51.50]	U	0.005	-0.569	0.019
HbA1c (%)	52	5.40 [5.30–5.53]	52	7.10 [6.70–7.50]	U	<0.001	3.025	<0.001
WBC (×10^3/μL)	52	6.86 [5.96–7.44]	52	8.22 [7.33–9.06]	U	<0.001	0.828	<0.001
RBC (×10^6/μL)	52	4.72 [4.36–5.08]	52	4.95 [4.75–5.12]	U	0.007	0.524	0.023
Hemoglobin (g/dL)	52	13.60 [12.85–15.07]	52	13.75 [13.12–15.27]	U	0.373	0.134	0.503
Platelets (×10^3/μL)	52	280.00 [229.75–297.00]	52	293.00 [249.00–331.50]	U	0.034	0.482	0.084
hs-CRP (mg/L)	52	1.58 [0.67–2.66]	52	5.61 [2.11–12.78]	U	<0.001	1.182	<0.001
CXCL1 (pg/mL)	52	73.70 [30.87–127.20]	52	101.32 [44.83–147.94]	U	0.428	0.16	0.525

Note: Continuous variables are presented as mean±SD or median [IQR]; categorical variables as n (%). Any p values equal to 0 are formatted as "<0.001" per journal style. Continuous variables are expressed as mean±SD or median [IQR], as appropriate; categorical variables as n (%). P values from independent-samples t-test or Mann–Whitney U, as appropriate. Abbreviations: BH - Benjamini-Hochberg adjusted q-value (FDR control); BMI - body mass index; BP - blood pressure; BUN - blood urea nitrogen; CXCL1 - C-X-C motif chemokine ligand 1; HbA1c - glycated hemoglobin; HDL-C - high-density lipoprotein cholesterol; Hedges g - standardized effect size between groups; hs-CRP - high-sensitivity C-reactive protein; LDH - lactate dehydrogenase; LDL-C - low-density lipoprotein cholesterol; RBC -red blood cell counts; T2DM - type 2 diabetes mellitus; WBC - white blood cell counts.

indices confirmed the diabetic phenotype with higher fasting and postprandial glucose, HbA1c, and insulin resistance (HOMA-IR) (Table 1). Additional baseline clinical and laboratory variables are provided in Table 1. Systemic inflammatory load was higher in T2DM reflected by substantially elevated hs-CRP ($p<0.001$) and modestly higher leukocyte counts ($p<0.001$). Circulating CXCL1 showed wide inter-individual variability and did not differ between groups ($p=0.428$) (Table 1).

In correlation analyses, CXCL1 related to adiposity- and inflammation-linked measures (BMI and hs-CRP), but not to fasting glucose, insulin, or HOMA-IR consistent with CXCL1 reflecting adiposity-related inflammation rather than glycemic status. To test whether CXCL1 adds discriminative information beyond standard clinical variables, we fit multivariable logistic models for MS and T2DM and quantified discrimination (AUC), calibration (slope/intercept, integrated calibration index [ICI], expected calibration error [ECE]), and internal validity using bootstrap correction and 5-fold cross-validation (Table 2, Figures 1–3).

For MS, adding CXCL1 to the base model produced a negligible change in discrimination (bootstrap-corrected $\Delta AUC=0.003$, $p=0.808$) and no

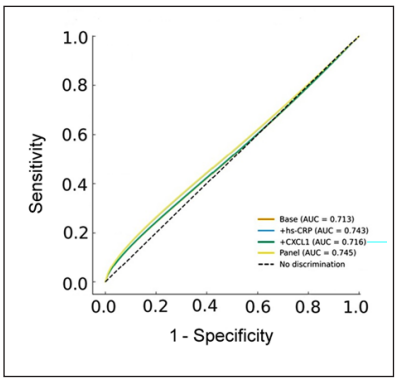

Figure 1. Receiver operating characteristic (ROC) curves for metabolic syndrome prediction models. Base model includes age, sex, and body mass index (BMI). Additional models include high-sensitivity C-reactive protein (hs-CRP) and C-X-C motif chemokine ligand 1 (CXCL1) individually and the combined biomarker panel. Dashed line represents no discrimination (AUC=0.5).

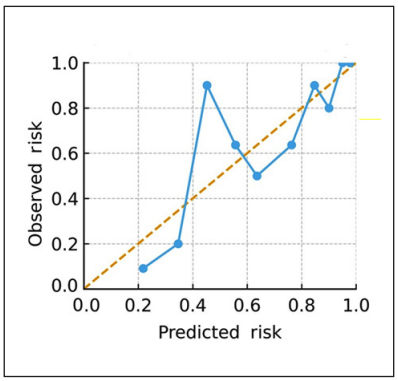

Figure 2. Calibration plot for metabolic syndrome prediction model. Observed probabilities are plotted against predicted risks across deciles of estimated probability. The dashed line represents perfect calibration (observed=predicted).

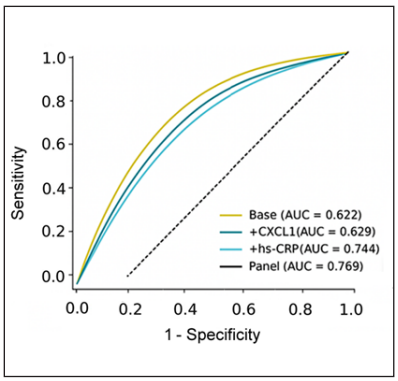

Figure 3. Receiver operating characteristic (ROC) curves for type 2 diabetes mellitus (T2DM) classification models. The base model includes age, sex, and body mass index (BMI). Additional models include C-X-C motif chemokine ligand 1 (CXCL1), high-sensitivity C-reactive protein (hs-CRP), and the combined biomarker panel. The dashed diagonal line indicates no discrimination (AUC=0.5).

Table 2
Comparative Model Performance for T2DM and MS

Endpoint	Model	Predictors	Apparent AUC	5-Fold CV AUC (mean±SD)	ΔAUC vs Base	Net Benefit (20%)
T2DM	Base	Age, Sex, BMI	0.622	0.588 ± 0.191	–	0.375
T2DM	+hs-CRP	Age, Sex, BMI, hs-CRP	0.744	0.706 ± 0.098	+0.118	0.388
T2DM	+CXCL1	Age, Sex, BMI, CXCL1	0.629	0.592 ± 0.185	+0.007	0.375
T2DM	Panel	Age, Sex, BMI, hs-CRP, CXCL1	0.769	0.716 ± 0.076	+0.128	0.394
MS	Base	Age, Sex, BMI	0.713	0.675 ± 0.139	–	0.331
MS	+hs-CRP	Age, Sex, BMI, hs-CRP	0.743	0.710 ± 0.116	+0.035	0.347
MS	+CXCL1	Age, Sex, BMI, CXCL1	0.716	0.678 ± 0.132	+0.003	0.332
MS	Panel	Age, Sex, BMI, hs-CRP, CXCL1	0.745	0.714 ± 0.111	+0.039	0.348

Comparative model performance for MS and T2DM including apparent AUC, cross-validated AUC, ΔAUC, and decision-curve net benefit at 20% threshold. Abbreviations: AUC – the area under the receiver operating characteristic curve; BMI – body mass index; CV – intra-assay coefficient of variation; CXCL1 – C-X-C motif chemokine ligand 1; hs-CRP – high-sensitivity C-reactive protein; MS – metabolic syndrome; SD – standard deviation; T2DM – type 2 diabetes mellitus.

clear independent association for CXCL1 (OR per 1 SD=1.48, 95% CI 0.82–2.67). Calibration remained acceptable (Figure 2).

For T2DM, CXCL1 likewise provided minimal incremental discrimination (ΔAUC=0.007, p=0.60) and no evidence of association (OR per 1 SD=0.97, 95% CI 0.63–1.50). Cross-validated AUCs and Brier scores were essentially unchanged after including CXCL1 (Table 2, Figure 3).

In contrast, substituting hs-CRP for CXCL1 improved model discrimination and net benefit modestly and the combined panel (age, sex, BMI, hs-CRP, CXCL1) yielded the highest apparent AUCs. However, optimism-adjusted gains were <0.01 indicating limited stable incremental information beyond standard predictors (Table 2, Figures 1–3).

Decision curve analysis showed small, threshold-dependent differences in net benefit across 10–30% intervention probabilities with no consistent clinical advantage from adding CXCL1 (Table 3). Subgroup and sensitivity analyses were consistent with the main findings including no effect modification by sex or BMI and similar results after excluding individuals with hs-CRP >10 mg/L. Overall, CXCL1 tracked inflammatory/adiposity burden, but did not independently improve discrimination, calibration, or clinical utility for MS or newly diagnosed T2DM beyond standard clinical variables and hs-CRP (Tables 1–3, Figures 1–3).

Table 3
ΔNB (+CXCL1 vs Base model [Age, Sex, BMI])

Phenotype	Threshold	Net Benefit (Base)	Net Benefit (+CXCL1)	ΔNB (vs Base)
MS	10%	0.626	0.626	0.000
MS	20%	0.584	0.587	+0.003
MS	30%	0.541	0.559	+0.018
T2DM	10%	0.444	0.444	0.000
T2DM	20%	0.358	0.358	0.000
T2DM	30%	0.291	0.269	−0.022

ΔNB values denote the difference versus the **base clinical model** (Age, Sex, BMI). Net benefit expressed on a 0–1 scale (per-patient basis; values ×100 = per-100 patients). At a 30% intervention threshold, inclusion of CXCL1 increased net benefit by ≈ 0.018 (1.8 %) relative to the base model. Abbreviations: BMI - body mass index; CXCL1 - C-X-C motif chemokine ligand 1; MS - metabolic syndrome; T2DM - type 2diabetes mellitus.

Discussion

This study examined whether circulating CXCL1 levels provide incremental discriminative value for MS or T2DM beyond standard anthropometric and inflammatory indices. Our primary endpoint was the classification of MS, while T2DM served as a secondary outcome for external comparison. In a cohort of newly diagnosed, treatment-naive individuals, CXCL1 correlated positively with adiposity and systemic inflammation, but failed to improve discrimination, calibration or clinical utility when incorporated into multivariable classification models. These findings suggest that although CXCL1 participates in the inflammatory network associated with metabolic dysregulation, its circulating concentration does not confer meaningful incremental discriminative value beyond established clinical and inflammatory markers, such as hs-CRP, in this cross-sectional setting. Our results, while statistically neutral, provide mechanistic clarity: CXCL1 behaves as a downstream effector within the adipose-inflammation axis rather than a driver of metabolic dysfunction.

The clustering of obesity, insulin resistance, and inflammation defines the MS a condition strongly linked to T2DM and cardiovascular disease (Eckel et al. 2005). Chronic low-grade inflammation has been recognized as a unifying pathophysiological mechanism across these disorders (Guria et al. 2023; Pellegrini et al. 2024). CXCL1 a chemokine ligand for CXCR2 mediates neutrophil chemotaxis and endothelial activation linking innate immune signaling to tissue remodeling (Korbecki et al. 2022; Lazennec et al. 2024). Experimental studies suggest that CXCL1 expression in adipose and vascular compartments is inducible by pro-inflammatory cytokines and metabolic stress (Lo et al. 2014; Korbecki et al. 2022). In animal models, increased CXCL1/CXCR2 signaling accompanies obesity and insulin resistance and CXCR2 antagonism can improve insulin sensitivity and attenuate vascular inflammation (Phillips et al. 2022; Lazennec et al. 2024). In human studies, circulating CXCL1 findings vary across cohorts and endpoints supporting a context-dependent interpretation rather than a robust standalone clinical marker (Korbecki et al. 2022).

In this study, CXCL1 correlated with BMI and hs-CRP, but not with fasting glucose, insulin, or HOMA-IR reinforcing its link to adiposity-related inflammation rather than glycemic status. Similar obesity-linked patterns have been described for other chemokines within metabolic inflammation networks (Wu and Ballantyne 2020; He et al. 2024). Mechanistically, CXCL1 release from differentiating adipocytes may be stimulated by irisin through NF-κB activation (Shaw et al. 2021) integrating

endocrine and inflammatory cues. Furthermore, CXCR2 regulation (desensitization, internalization, and recycling) can modify ligand kinetics and attenuate the relationship between circulating CXCL1 and tissue-level activity (Sitaru et al. 2023; Lazennec et al. 2024; Toya et al. 2024), which may help explain limited discriminative performance despite underlying inflammation.

Discrimination was assessed via AUC and cross-validation, calibration via the Integrated Calibration Index (ICI) and related metrics and clinical utility via decision curve analysis (Table 3). These approaches are supported by contemporary guidance for model evaluation and transparent reporting (Vickers et al. 2016; Austin and Steyerberg 2019; Austin et al. 2020; Collins et al. 2024). The finding that CXCL1 did not improve AUC, calibration or net benefit underscores the limited incremental value of isolated cytokine markers in discriminative modeling. This aligns with growing advocacy for integrative, multi-marker or systems level frameworks rather than reliance on single analytes (Hu and Jia 2021; Moin et al. 2021; Ion et al. 2025). Our logistic regression models showed acceptable discrimination and calibration for both MS and T2DM under current reporting guidance (Austin and Steyerberg 2019; Austin et al. 2020; Collins et al. 2024).

The relatively higher apparent AUC compared to the cross-validated estimate suggests moderate optimism, likely reflecting small-sample variability rather than substantive overfitting. The 5-fold CV AUC, due to its internal resampling design, represents a more conservative and thus reliable estimate of discriminative performance. These findings collectively support the robustness of the results while acknowledging the inherent limitations of small-sample discriminative modeling.

Notably, hs-CRP consistently demonstrated superior discrimination and net benefit compared with CXCL1 across both metabolic outcomes. hs-CRP, a hepatically synthesized acute-phase reactant regulated by inflammatory cytokines captures global inflammatory tone and integrates diverse upstream signaling cascades (Kim and Lim 2022; Pellegrini et al. 2024). The ROC results confirmed that CXCL1 added only threshold-dependent minimal clinical benefit, whereas hs-CRP yielded measurable net gains in decision-making across relevant intervention probabilities. These observations emphasize the translational distinction between mechanistic biomarkers and clinically deployable predictors. While CXCL1 may contribute biologically to inflammation in metabolic disease, its analytic variability and narrow signal window reduce its utility as a stand-alone clinical tool.

The subtle context-dependent behavior of CXCL1 under heightened inflammatory burden (e.g., high hs-CRP) could reflect feedback regulation of synthesis, altered clearance or shifts within the broader CXC chemokine network (Korbecki et al. 2022; Lazennec et al. 2024). CXCR2 expression and signaling can also be modulated by persistent inflammatory stimuli potentially altering ligand kinetics and downstream effects (Sitaru et al. 2023). These hypotheses warrant mechanistic exploration using longitudinal and tissue-specific models.

Methodologically, the present study has several strengths. All participants were treatment-naive, minimizing drug-induced modulation of inflammatory markers. Laboratory assays were standardized; key pre-analytical considerations known to affect cytokine quantification were controlled (Liu et al. 2021). Model development and reporting followed best-practice recommendations with internal validation and calibration assessment (Vickers et al. 2016; Austin and Steyerberg 2019; Austin et al. 2020; Collins et al. 2024). Several limitations should be acknowledged. The cross-sectional design precludes causal inference, and the modest sample size (n=104) limits power to detect small interaction effects. Circulating CXCL1 may not fully reflect local adipose or vascular activity due to compartmentalization and CXCR2 dynamics (Korbecki et al. 2022; Lazennec et al. 2024; Toya et al. 2024). Finally, the relatively homogeneous study population may limit generalizability. In future, multicenter longitudinal studies integrating molecular and functional readouts are warranted.

Preclinical studies in high-fat diet and genetic mouse models have shown that CXCL1/CXCR2 signaling can contribute to adipose inflammation, immune-cell recruitment, and insulin resistance, and that CXCR2 antagonism may improve metabolic phenotypes (Phillips et al. 2022; Sitaru et al. 2023; Lazennec et al. 2024). However, translating these mechanistic findings to human physiology remains challenging. Our results suggest that while CXCL1 may be active at the tissue level, circulating concentrations in humans more likely reflect downstream inflammatory activity rather than a primary pathogenic signal (Sajadi et al. 2013; Korbecki et al. 2022). This contrast underscores the need for longitudinal human studies integrating molecular and systems-level biomarkers (Hu and Jia 2021; Moin et al. 2021; Ion et al. 2025).

From a translational perspective, these findings emphasize the importance of multi-marker and

systems-level approaches. CXCL1 may serve as one component within integrated inflammatory signatures, contributing to individualized risk profiling when contextualized alongside broad markers such as hs-CRP (Hu and Jia 2021; Moin et al. 2021; Ion et al. 2025). Integration of CXCL1 into multiplex or network-based biomarker frameworks may uncover interactions not evident in isolated analyses. CXCL1 reflects adiposity-associated inflammation and provides minimal incremental discriminative value for MS or newly diagnosed T2DM once conventional risk factors and hs-CRP are considered. This supports the inflammation-related biomarkers interpretation within a network context rather than as standalone biomarkers.

Conclusion

In treatment of naive individuals with newly diagnosed T2DM, CXCL1 reflects adiposity-driven inflammation, but provides limited standalone incremental discriminative value. Its context-dependent behavior under higher inflammatory load may still inform integrated multi-marker frameworks that aim to improve metabolic phenotype classification. Future longitudinal and multi-omics studies are needed to test whether CXCL1 adds value to prospective risk assessment when evaluated alongside broader inflammatory markers.

Acknowledgments

The authors thank the Biochemistry Laboratory team at Izmir Bozyaka Training and Research Hospital for technical assistance during sample processing.

Conflicts of interest: *Authors declare no conflict of interest.*

References

Alberti KG, Eckel RH, Grundy SM, Zimmet PZ, Cleeman JI, Donato KA, Fruchart JC, James WP, Loria CM, Smith SC Jr. Harmonizing the metabolic syndrome: a joint interim statement of the International Diabetes Federation Task Force on Epidemiology and Prevention; National Heart, Lung, and Blood Institute; American Heart Association; World Heart Federation; International Atherosclerosis Society; and International Association for the Study of Obesity. Circulation 120, 1640–1645, 2009.

Austin PC, Steyerberg EW. The Integrated Calibration Index (ICI) and related metrics for quantifying the calibration of logistic regression models. Stat Med 38, 4051–4065, 2019.

Austin PC, Harrell FE Jr, van Klaveren D. Graphical calibration curves and the integrated calibration index (ICI) for survival models. Stat Med 39, 2714–2742, 2020.

Collins GS, Moons KGM, Dhiman P, Riley RD, Beam AL, Van Calster B, Ghassemi M, Liu X, Reitsma JB, van Smeden M, Boulesteix AL, Camaradou JC, Celi LA, Denaxas S, Denniston AK, Glocker B, Golub RM, Harvey H, Heinze G, Hoffman MM, Kengne AP, Lam E, Lee N, Loder EW, Maier-Hein L, Mateen BA, McCradden MD, Oakden-Rayner L, Ordish J, Parnell R, Rose S, Singh K, Wynants L, Logullo P. TRIPOD+AI statement: updated guidance for reporting clinical prediction models that use regression or machine learning methods. BMJ 385, e078378, 2024.

Eckel RH, Grundy SM, Zimmet PZ. The metabolic syndrome. Lancet 365, 1415–1428, 2005.

ElSayed NA, Aleppo G, Aroda VR, Bannuru RR, Brown FM, Bruemmer D, Collins BS, Hilliard ME, Isaacs D, Johnson EL, Kahan S, Khunti K, Leon J, Lyons SK, Perry ML, Prahalad P, Pratley RE, Seley JJ, Stanton RC, Gabbay RA. Classification and diagnosis of diabetes: Standards of Care in Diabetes—2023. Diabetes Care 46, S19–S40, 2023.

Guria S, Hoory A, Das S, Chattopadhyay D, Mukherjee S. Adipose tissue macrophages and their role in obesity-associated insulin resistance: an overview of the complex dynamics at play. Biosci Rep 43, BSR20220200, 2023.

He W, Wang H, Yang G, Zhu L, Liu X. The role of chemokines in obesity and exercise-induced weight loss. Biomolecules 14, 1121, 2024.

Hu C, Jia W. Multi-omics profiling: the way towards precision medicine in metabolic diseases. J Mol Cell Biol 13, 576–593, 2021.

Ion G, Bostan M, Hardman WE, Putt McFarland M, Bleotu C, Radu N, Diaconu CC, Mihaila M, Caramihai MD, Hotnog CM. Nutrients lowering obesity-linked chemokines blamable for metastasis. Int J Mol Sci 26, 2275, 2025.

Kim JH, Lim JS. The association between C-reactive protein, metabolic syndrome, and prediabetes in Korean children and adolescents. Ann Pediatr Endocrinol Metab 27, 273–280, 2022.

Korbecki J, Gassowska-Dobrowolska M, Wojcik J, Szatkowska I, Barczak K, Chlubek M, Baranowska-Bosiacka I. The importance of CXCL1 in physiology and noncancerous diseases of bone, bone marrow, muscle and the nervous system. Int J Mol Sci 23, 4205, 2022.

Lazennec G, Rajarathnam K, Richmond A. CXCR2 chemokine receptor - a master regulator in cancer and physiology. Trends Mol Med 30, 37–55, 2024.

Liu C, Chu D, Kalantar-Zadeh K, George J, Young HA, Liu G. Cytokines: from clinical significance to quantification. Adv Sci 8, e2004433, 2021.

Lo HM, Lai TH, Li CH, Wu WB. TNF-α induces CXCL1 chemokine expression and release in human vascular endothelial cells in vitro via two distinct signaling pathways. Acta Pharmacol Sin 35, 339–350, 2014.

Moin ASM, Sathyapalan T, Diboun I, Atkin SL, Butler AE. Identification of macrophage activation-related biomarkers in obese type 2 diabetes that may be indicative of enhanced respiratory risk in COVID-19. Sci Rep 11, 6428, 2021.

Monickaraj F, Acosta G, Cabrera AP, Das A. Transcriptomic profiling reveals chemokine CXCL1 as a mediator for neutrophil recruitment associated with blood-retinal barrier alteration in diabetic retinopathy. Diabetes 72, 781–794, 2023.

Pan X, Tan X, McDonald J, Kaminga AC, Chen Y, Dai F, Qiu J, Zhao K, Peng Y. Chemokines in diabetic eye disease. Diabetol Metab Syndr 16, 115, 2024.

Pellegrini V, La Grotta R, Carreras F, Giuliani A, Sabbatinelli J, Olivieri F, Berra CC, Ceriello A, Prattichizzo F. Inflammatory trajectory of type 2 diabetes: novel opportunities for early and late treatment. Cells 13, 1662, 2024.

Phillips BE, Lantier L, Engman C, Garciafigueroa Y, Singhi A, Trucco M, Mantzoros C, Wasserman D, Giannoukakis N. Improvement in insulin sensitivity and prevention of high fat diet-induced liver pathology using a CXCR2 antagonist. Cardiovasc Diabetol 21, 130, 2022.

Sajadi SM, Khoramdelazad H, Hassanshahi G, Rafatpanah H, Hosseini J, Mahmoodi M, Arababadi MK, Derakhshan R, Hasheminasabzavareh R, Hosseini-Zijoud SM, Ahmadi Z. Plasma levels of CXCL1 (GRO-alpha) and CXCL10 (IP-10) are elevated in type 2 diabetic patients: evidence for the involvement of inflammation and angiogenesis/angiostasis in this disease state. Clin Lab 59, 133–137, 2013.

Shaw A, Toth BB, Kiraly R, Arianti R, Csomos I, Poliska S, Vamos A, Korponay-Szabo IR, Bacso Z, Gyory F, Fesus L, Kristof E. Irisin stimulates the release of CXCL1 from differentiating human subcutaneous and deep-neck derived adipocytes via upregulation of NFκB pathway. Front Cell Dev Biol 9, 737872, 2021.

Sitaru S, Budke A, Bertini R, Sperandio M. Therapeutic inhibition of CXCR1/2: where do we stand? Intern Emerg Med 18, 1647–1664, 2023.

Sun H, Saeedi P, Karuranga S, Pinkepank M, Ogurtsova K, Duncan BB, Stein C, Basit A, Chan JCN, Mbanya JC, Pavkov ME, Ramachandaran A, Wild SH, James S, Herman WH, Zhang P, Bommer C, Kuo S, Boyko EJ, Magliano DJ. IDF Diabetes Atlas: global, regional and country-level diabetes prevalence estimates for 2021 and projections for 2045. Diabetes Res Clin Pract 183, 109119, 2022.

Toya S, Struyf S, Huerta L, Morris P, Gavioli E, Minnella EM, Cesta MC, Allegretti M, Proost P. A narrative review of chemokine receptors CXCR1 and CXCR2 and their role in acute respiratory distress syndrome. Eur Respir Rev 33, 230172, 2024.

Vickers AJ, Van Calster B, Steyerberg EW. Net benefit approaches to the evaluation of prediction models, molecular markers, and diagnostic tests. BMJ 352, i6, 2016.

Wu H, Ballantyne CM. Metabolic inflammation and insulin resistance in obesity. Circ Res 126, 1549–1564, 2020.

Zlotnik A, Yoshie O. Chemokines: a new classification system and their role in immunity. Immunity 12, 121–127, 2000.